ASME Journal of Engineering for Gas Turbines and Power
Online journal at:
https://asmedigitalcollection.asme.org/gasturbinespower

Reacting Flow Prediction of the Low-Swirl Lifted Flame in an Aeronautical Combustor With Angular Air Supply

Sven Hoffmann[1]
Institut für Thermische Strömungsmaschinen,
Karlsruher Institut für Technologie (KIT),
Kaiserstr. 12,
Karlsruhe 76131, Germany
e-mail: sven.hoffmann@kit.edu

Rainer Koch
Institut für Thermische Strömungsmaschinen,
Karlsruher Institut für Technologie (KIT),
Kaiserstr. 12,
Karlsruhe 76131, Germany

Hans-Jörg Bauer
Institut für Thermische Strömungsmaschinen,
Karlsruher Institut für Technologie (KIT),
Kaiserstr. 12,
Karlsruhe 76131, Germany

The development of lean-burn combustion systems is of paramount importance for reducing the pollutant emissions of future aero engine generations. By tilting the burners of an annular combustor in circumferential direction relative to the rotational axis of the engine, the potential of increased combustion stability is opened up due to an enhanced exhaust gas recirculation between adjacent flames. The innovative gas turbine combustor concept, called the short helical combustor (SHC), allows the main reaction zone to be operated at low equivalence ratios. To exploit the higher stability of the fuel-lean combustion, a low-swirl lifted flame is implemented in the staggered SHC burner arrangement. The objective is to reach ultralow NO_x emissions by complete evaporation and extensive premixing of fuel and air upstream of the lean reaction zone. In this work, a modeling approach is developed to investigate the characteristics of the lifted flame in an enclosed single-burner configuration, using the gaseous fuel methane. It is demonstrated that by using the large eddy simulation method, the shape and liftoff height of the flame are adequately reproduced by means of the finite-rate chemistry approach. For the numerical prediction of the lean lifted flame in the SHC arrangement, the focus is on the interaction of adjacent burners. It is shown that the swirling jet flow is deflected toward the sidewall of the staggered combustor dome, which is attributed to the asymmetrical confinement. Since the stabilization mechanism of the low-swirl flame relies on outer recirculation zones, the upstream transport of hot combustion products back to the flame base is studied by the variation of the combustor confinement ratio. It turns out that increasing the combustor size amplifies the exhaust gas recirculation along the sidewall, and increases the temperature of recirculating burned gases. This study emphasizes the capability of the proposed lean-burn combustor concept for future aero engine applications. [DOI: 10.1115/1.4063988]

1 Introduction

In order to mitigate the environmental impact of civil aviation and meet the stringent legislative regulations in the future, the pollutant emissions from aircraft propulsion systems must be substantially reduced. Hence, the development of low-emission aero engine combustors is crucial for reaching the ambitious long-term emission targets defined by, among others, ACARE Flightpath 2050 [1].

High thermal efficiencies can be reached by increasing the combustor temperature and the overall pressure ratio, which in turn reduces the emission of carbon dioxide (CO_2) attributed to less fuel burn. Elevated temperatures and air pressures, furthermore, enable complete combustion due to fast chemical reactions, resulting in low emissions of carbon monoxide (CO) and unburned hydrocarbons. However, the formation of nitrogen oxides (NO_x) is amplified at high temperatures since the formation rate of the prevalent thermal NO does exponentially rise with the flame temperature. NO_x emissions can thus be reduced by controlling the stoichiometry to limit the maximum temperature at high-power conditions [2].

In recent years, different gas turbine combustion technologies aiming at low emissions have been developed, e.g., Rich burn–Quick quench–Lean burn, axially or radially staged concepts, lean direct injection and lean premixed prevaporized (LPP) [3–5]. Among these, the lean-burn systems promise significant NO_x reduction levels due to lower flame temperatures achieved by operating the combustion zone under fuel-lean conditions using excess air.

In the case of the lean direct injection concept, the fuel is directly injected into the reaction zone, and provided that the fuel is quickly evaporated and mixed with air, near-stoichiometric conditions causing high-temperature spots can be avoided [6]. Achieving fine atomization and rapid fuel–air mixing are the main design challenge which is posed to the fuel injection system. In addition, combustor staging or piloting is prerequisite due to insufficient lean blow-out (LBO) stability at lower load conditions to avoid weak flame extinction. However, both measures will increase the NO_x emissions [3]. The operating principle of the LPP concept is to feed the

Turbomachinery Technical Conference & Exposition, Hynes Convention Center, June 26–30, 2023. Turbo Expo 2023.
[1]Corresponding author.
Manuscript received July 26, 2023; final manuscript received September 8, 2023; published online January 12, 2024. Editor: Jerzy T. Sawicki.

combustion zone with a homogeneous mixture of fuel and air at a low equivalence ratio, yielding uniformly low temperatures, and thus reducing NO_x drastically. The major drawback of the LPP concept is the inherent risk of auto-ignition and flashback inside the injection system due to the long residence time required for evaporation and premixing. Furthermore, the combustor is prone to thermo-acoustic combustion instabilities [7].

In order to remedy the shortcomings of the previously discussed lean-burn combustor concepts, a novel combustor design is proposed in the CHAiRLIFT project under the European research program Clean Sky 2 Joint Undertaking. The unique design involves the short helical combustor (SHC) concept, which is an annular combustor with angular air supply, and lean lifted flames induced by a low-swirl injector nozzle. The principal constructional characteristic of this combustor is the tilting of the burners in circumferential direction with respect to the rotor axis of the engine. This particular arrangement is expected to increase the flame stability by the enhanced interaction between the fresh reactants and the exhaust gases of adjacent burners, ensuring safe and reliable operation in lean combustion mode. Furthermore, NO_x emissions are reduced due to the premixing of fuel and air upstream of the reaction zone of the lifted flames.

In Fig. 1, the SHC concept is schematically shown. The air flow coming from the compressor features a tangential velocity component which leads to a helical flow pattern, allowing the axial length of the combustor to be reduced. Consequently, the overall weight of the engine decreases, and the mechanical integrity of the engine core can be improved. Furthermore, the number of nozzle guide vanes is reduced since a lower deflection in the turbine vane stage is required by exploiting the angular momentum of the helical flow. This in turn leads to a reduction of aerodynamic losses and cooling air requirements. The SHC arrangement was numerically investigated by Ariatabar et al. [9–11] focusing on the fundamental aerothermal characteristics of high-swirl flames. It was demonstrated that a double annular configuration with a burner tilting angle of 45 deg is most beneficial with respect to a homogeneous recirculation zone of the swirl flames, and an uniform flow and temperature pattern at the combustor exit. In a similar study of Hu et al. [12], the tilting angle of a high-swirl single annular configuration was varied. It was found that the exchange of mass and energy between adjacent recirculation zones of the reactive flow field is reduced for higher tilting angles.

Besides the tilting of the burners, the key feature of the intended novel combustor concept is the integration of lean lifted flames. In general, lifted flames burn in a liftoff regime, which provides a premixing zone for the fresh reactants upstream of the flame front. This will reduce the occurrence of hot spots, and thus NO_x emissions for lean reactant mixtures if a high degree of fuel–air homogeneity is achieved [13]. The liftoff behavior has been largely studied in the literature for turbulent free-jet diffusion flames [14], including partially premixing [15] and coflowing air [16]. For the proposed concept, a confined low-swirl lifted flame is considered, which represents a practical application for gas turbine combustors [17]. This type of flame has been extensively investigated in several experimental studies of an enclosed single-burner configuration [18–20], using a particular low-swirl injector design proposed by Zarzalis et al. [21]. In Fig. 2, the schematic of the lifted flame burner used for these studies is shown. The airflow through the nozzle is swirled only in the inner primary swirler, whereas in the outer secondary part, no swirl is imposed. This specific setup leads to the flame being detached from the injector, establishing the liftoff zone between the nozzle and the main combustion zone. Consequently, the fuel evaporation and the mixing of the reactants are promoted directly inside the combustor without the requirement of premixing ducts. In this way, local near-stoichiometric conditions, and thus high temperatures in the partially premixed flame can be avoided which typically cause an increased formation of NO_x emissions. At the same time, the susceptibility to flashback and thermo-acoustic instabilities are limited [19]. The upstream propagation of the flame into the burner is inhibited since the fuel and air first interact in the combustor [23]. The flame is controlled by the characteristic flow field featuring a weak inner recirculation zone which enhances the mixing of the primary and secondary flow, and an outer recirculation zone (ORZ) providing the dominant stabilization mechanism. By the upstream transport of exhaust gases from the reaction zone back to the flame base, the hot combustion products are mixed into the swirling jet, ensuring the continuous re-ignition of the incoming fresh gases. The propagating premixed-like flame front is stabilized at the downstream position of the liftoff height (LOH) where the flame speed is in balance with the flow velocity. The LOH plays a key role for the NO_x reduction potential because it determines the mixing time of fuel and oxidizer before entering the reaction zone. Hence, in the previous experimental campaigns, the impact of various operating conditions and geometric features on the LOH was investigated.

In addition to the experimental studies, numerical predictions of the lifted flame characteristics have been performed using computational fluid dynamics (CFD). The prediction of the complex flame liftoff process is generally challenging since it requires the modeling of finite-rate chemistry effects and turbulent mixing to capture the ignition and flame stabilization adequately. In regard to CFD, the scale-resolving large eddy simulation (LES) approach has proven to

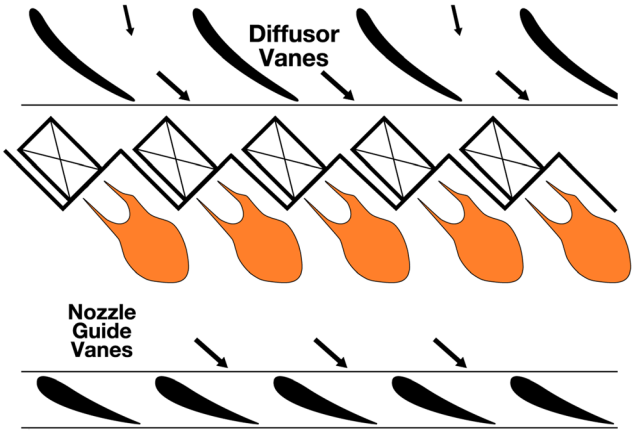

Fig. 1 Conceptual sketch of the short helical combustor adapted from Ref. [8]

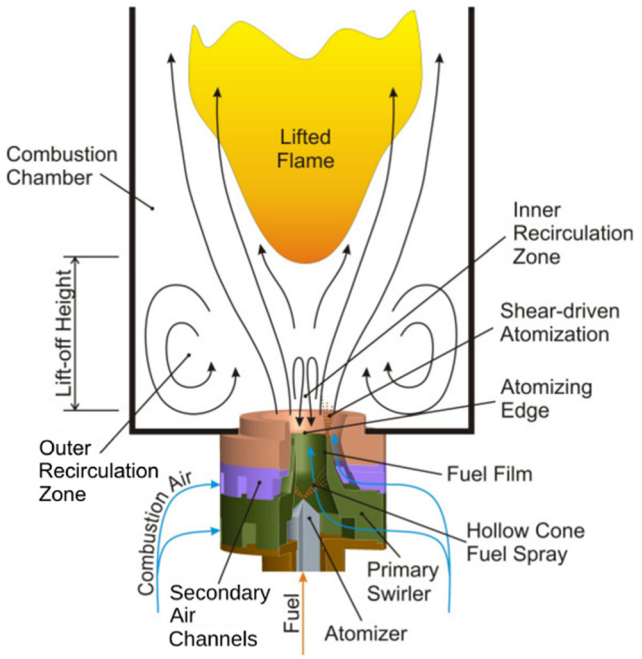

Fig. 2 Schematic of the lifted flame burner adapted from Ref. [22]

be an efficient and accurate method for the simulation of reacting flows in the context of gas turbine combustion [24]. By using the turbulent flamelet model [25] or the flamelet-generated manifold approach [26,27] combined with a presumed probability density function closure method to describe turbulence–chemistry interaction, the overall reactivity of the low-swirl lifted flame was overpredicted, giving smaller liftoff heights compared to the experimental findings. In contrast, the thickened flame model slightly overestimated the position of the main reaction zone by using a global two-step reaction mechanism [28]. In the recent numerical study of this flame, a coupled thickened flame-flamelet-generated manifold approach was implemented, which improved the prediction of the liftoff and flame shape at moderate computational costs [29].

The CHAiRLIFT combustor design was numerically investigated by the authors [30] with respect to isothermal flow characteristics. It was found that the low-swirl jet significantly interacts with the sidewall of the staggered SHC concept, leading to the deflection of the flow toward the sidewall due to an asymmetric pressure field in the vicinity of the burner. By means of a parametric study of nozzle characteristics and combustor dimensions, it was shown that an increased confinement ratio between the flame tube and the swirl nozzle strongly enhances the outer recirculation, which would be beneficial for the stability of the lifted flame. Furthermore, a linear multi-burner arrangement consisting of five burners was erected by Shamma et al. [31] to investigate the interaction of adjacent spray flames in the inclined configuration. In the experiment, it was proven that a remarkable high LBO limit for nonpiloted burners is achievable. This could be attributed to the transfer of hot exhaust gases to the flame base of the neighboring burner, featuring the essential stabilization mechanism of the lifted flames. In complementary numerical studies of Langone et al. [32], the tilting angle of the multi-burner arrangement was varied, providing more insights into the complex three-dimensional hot-gas recirculation. It was concluded that a tilting angle of the burners between 20 deg and 30 deg could lead to better flame stability since this range reflects a favorable compromise between the extent and the averaged temperature of the recirculation zone.

In this work, LES reacting flow predictions of the low-swirl lifted methane-air flame inside the helical burner arrangement of the SHC are presented. By including turbulent combustion, this study extends the previous work of the authors which established an understanding of the aerodynamics of the tilted burners, and highlighted the impact of nozzle and combustor features on the nonreacting flow. To this end, a simulation methodology is developed which allows for the accurate prediction of the lifted flame characteristics. The objective is to investigate the reactive flow field of this novel combustor concept with respect to the flame stabilization mechanism. Hence, special emphasis is put on the exhaust gas recirculation between the flames due to the interaction of adjacent burners, providing a preheating of the fresh mixture, and thus ensuring flame stability. Furthermore, the impact of the geometric combustor confinement on the flow field and flame position is studied, aiming at the optimization of the concept in terms of enhanced hot-gas recirculation. For the simulations performed in this conceptual study, only gaseous methane is used in order to reduce the complexity of the modeling. At high preheating temperatures, the flame liftoff behavior of the gaseous and liquid fuel combustion is very similar [20]. This is attributed to the spray being completely evaporated close to the nozzle, and the fuel–air flow featuring the same state of premixing as for gaseous fuel [19].

First, the dedicated numerical model facilitating the prediction of the lifted flame is presented. It is validated using the experimental results of the single-burner configuration. The features of the lifted flame of the SHC reference case are discussed afterward. Finally, the geometric combustor confinement ratio is varied by adjusting the flame tube height.

2 Validation of Combustion Modeling

In this section, the numerical model developed for the prediction of the low-swirl lifted flame is validated. To this end, the experimental test case of the enclosed single-burner is numerically reproduced. The study of the lifted flame in the single-burner highlights the importance of the outer recirculation zone for the stabilization mechanism due to the interaction of the swirling jet with confining combustor walls.

2.1 Experimental Test Case. The concept of the low-swirl lifted flame has been investigated in different experimental works in the previous years [18–20]. In this study, the single-burner configuration of Sedlmaier et al. [20,26] is taken as the reference. The fuel injector used (see Fig. 2) is based on the principle of airblast atomization, and it can be operated with both liquid and gaseous fuels. The effective area of the nozzle outlet is 131 mm^2 as determined in Ref. [20]. Swirl is imposed to the flow only in the inner primary swirler featuring a theoretical swirl number of 0.76. Since a greater amount of air enters the outer secondary channels where it is not swirled, the total swirl number of the flow issued from the nozzle is well below the critical value of the vortex breakdown, which is in the range of 0.4–0.6 [33]. In contrast to conventional swirl-stabilized flames, this specific low-swirl arrangement results in a small inner recirculation zone in the shear layer between the primary and secondary flow, but without exhaust gas entrainment, allowing the flame to be lifted off and stabilized by the outer hot-gas recirculation. The inner diameter of the cylindrical combustion chamber is 89 mm and the length is 320 mm, and it is made from quartz glass providing optical accessibility. Furthermore, the flame tube is externally cooled by a predefined constant cooling air flow. Further details about the experimental test rig and the applied measurement techniques can be found in Refs. [20] and [26].

In the experiment, the operating conditions have been widely varied to investigate the impact on the lifted flame characteristics. The operating point which is selected for the numerical predictions in this work features an air preheating temperature of $T_0 = 573$ K, a pressure of $p = 4$ bar, a relative pressure drop across the injector of $\Delta p/p_0 = 3\%$, and an overall equivalence ratio for the methane-air mixture of $\phi = 0.53$.

In Fig. 3, experimental measurements of the OH* chemiluminescence and the OH planar laser-induced fluorescence are shown. By means of the OH* intensity map, the main reaction zone can be identified, revealing the typical arrow-shaped form of the flame [18]. In addition, the time-averaged OH* distribution is used to calculate the liftoff height which is defined as the streamwise position where 10% of the integral intensity is reached. The instantaneous OH intensity map reveals that there are already pockets of reacting mixture in the premixing zone, yet the flame cannot stabilize there

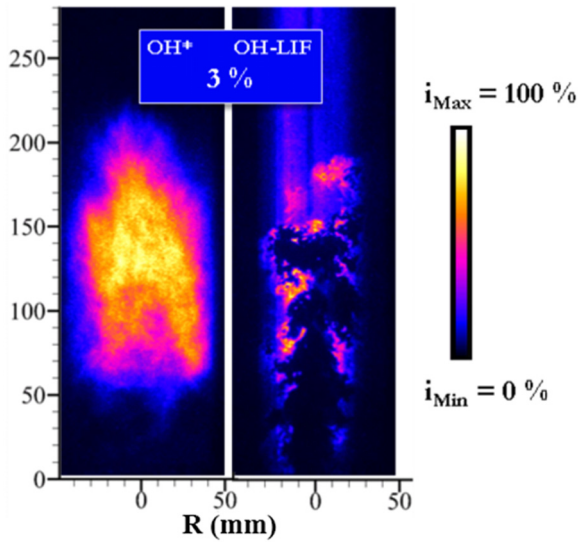

Fig. 3 OH* chemiluminescence and planar OH-LIF measurements adapted from Ref. [26]

due to the high flow velocities in that region. Both the OH* and OH light emission intensities will be used for the comparison of the simulation to the experiment regarding the shape and extent of the flame, and the liftoff height.

2.2 Numerical Model. The reacting flow solver *reactingFoam* of the open-source CFD software OPENFOAM v7 [34] is used for the turbulent combustion simulation of the lifted flame. It is a pressure-based solver which incorporates reaction kinetics to calculate the chemical source terms in the species transport equations. The numerical time-step of the transient predictions is 2×10^{-6} s, keeping the maximum CFL number in the combustor below the value of 1. For the time averaging of flow quantities, a physical time span of 140 ms is covered. The spatial and temporal discretization are performed by using second-order numerical schemes.

The geometry of the single-burner configuration is adopted for the simulation, whereas the low-swirl nozzle is not included in the numerical model to reduce the simulation effort. The computational domain of the cylindrical combustor is shown in Fig. 4. Since the nozzle is not part of the model, the circular inlet patch of the domain at the bottom of the flame tube represents the outlet cross section of the nozzle. A contraction is attached to the end of the combustor in order to prevent undesired backflow effects at the outlet, and ensure numerical stability. The combustor is discretized by a block-structured OH-type mesh consisting of 2.4 M hex elements, providing reduced numerical diffusion due to the low level of skewness and nonorthogonality of the cells.

To establish the characteristic flow field of the low-swirl jet, distinct profiles are imposed at the inlet patch as fixed value boundary conditions. In Fig. 4, the profiles of the species mass fractions Y_k of methane and air including oxygen, nitrogen, argon, and helium, the temperature T and the velocity components u_i are shown. These inlet profiles represent time-averaged fields, and were extracted from reactive LES predictions of the lifted methane flame performed by Langone et al. [27], in which the complete geometry of the nozzle was included. The profiles were extracted at the position of the nozzle outlet coinciding with the inlet patch of the present model. The approach of using such inlet profiles was also followed for accurately predicting the nonreacting low-swirl flow of the single-burner [31], and the spray flames of the multi-burner arrangement [32].

The formulation of inlet conditions for LES is a complicated task because the inlet flow must include a component of stochastic variation while meeting different requirements, with the correct turbulent energy spectrum being highly significant. In that regard, the methods of precursor simulations and synthesized turbulence are suggested [35]. Besides the mean velocity profiles originating from

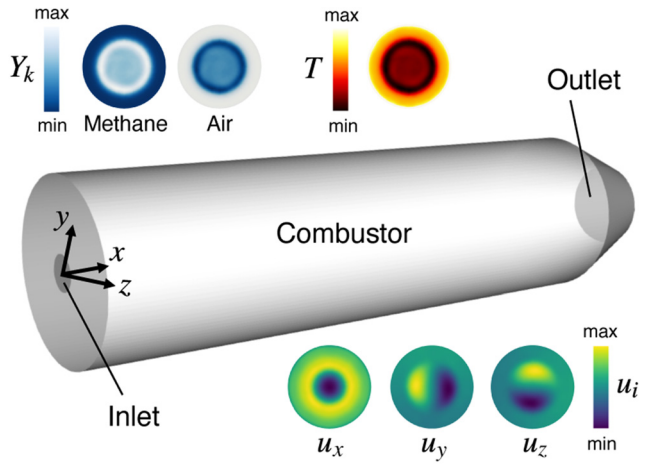

Fig. 4 Computational domain of the single-burner and inlet profiles for species mass fractions, temperature, and velocity components

the precursor LES, a synthetic inflow-turbulence generator implemented by Galeazzo et al. [36] is used here. The turbulence generator is based on the digital filtering of random noise [37], which implies the correlated spatial and temporal fluctuation of the turbulent structures. Thereby, coherent velocity fluctuations are superimposed to the mean flow profiles at the inlet, reflecting the natural energy spectrum of a turbulent flow. Furthermore, the wall-adapting local eddy-viscosity turbulence model [38] is used to account for the subgrid-scale stresses which are not resolved by the LES low-pass filtering operation.

The operating pressure of 4 bar is prescribed at the outlet of the computational domain, and the no-slip condition is imposed on the combustor walls. In addition, a thermal boundary condition is enforced at the lateral wall of the cylindrical flame tube by imposing a uniform wall temperature of 1200 K to consider the wall heat losses due to the external cooling in the experiment. An estimation of the wall heat losses is given in Ref. [26], yet no wall temperatures are reported. Using a uniform combustor wall temperature for this configuration was also followed in the works of Langone et al. [27–29].

The reduced chemical kinetic mechanism KEE for the combustion of methane-air mixtures as proposed by Kee et al. [39] is used. This skeletal mechanism lowers significantly the computational costs compared to a detailed chemical kinetic model, but includes multiple intermediate reaction steps and transient species unlike global reaction mechanisms. In this study, the KEE mechanism is extended by a submechanism to predict the formation of electronically excited OH* molecules [40], which enables the comparison of the lifted flame characteristics to the experimental data. A total of 20 species and 72 reactions are involved to describe the reaction kinetics. Besides oxygen and nitrogen, the combustion air includes argon as another collisional partner for the quenching of OH* molecules, and helium as the inert species to ensure mass conservation in the numerical procedure. In the finite-rate chemistry approach, a scalar transport equation of the filtered mass fraction $\tilde{Y}_k$ is solved for each species k. The formation rates $\dot{\omega}_k$ as the chemical source terms representing the evolution of each species mass fraction are computed by solving the coupled nonlinear ordinary differential equation (ODE) system of chemical kinetics.

A turbulent combustion model is required to close the turbulence–chemistry interaction problem arising mathematically from the LES filter operation. In this study, the reactor-based partially stirred reactor (PaSR) model [41] is employed. It is based on the idea that each computational cell is partitioned into the perfectly stirred zone of reacting fine structures and the surrounding nonreacting zone driven by turbulent mixing. After the chemical reactions have taken place, the combustion products are mixed with the unburned surroundings due to turbulence. Based on this decoupling of the reaction and the turbulent mixing, the overall reaction progress is determined by the mass exchange between the two zones. The fraction of the cell which is occupied by the chemical reactions is the reacting volume fraction κ which reads

$$\kappa = \frac{\tau_c}{\tau_c + \tau_{mix}} \tag{1}$$

where τ_c and τ_{mix} are the characteristic time scales of the chemical reactions and the turbulent mixing, respectively. The estimation of these time scales is crucial to obtain accurate predictions from the model, for which various formulations are available in the literature [42]. In this work, the definitions which are implemented in the standard OpenFOAM [34] code are used. At last, the unclosed filtered chemical reaction rate $\overline{\dot{\omega}}_k$ in the species transport equation can be calculated from the formation rate based on filtered flow quantities by using the reacting volume fraction by means of

$$\overline{\dot{\omega}}_k = \kappa\, \dot{\omega}_k(\tilde{\mathbf{Y}}, \tilde{T}) \tag{2}$$

Recently, the computational efficient PaSR model has been widely used for the numerical investigation of MILD combustion

applications [42,43] featuring strong interactions between the chemical kinetics and turbulent mixing phenomena, also governing the low-swirl lifted flame of this work.

Due to the highly nonlinear nature of the chemical kinetics represented by the stiff ODE system, the convergence rate of the ODE temporal integrators computing the source terms in each grid cell can vary significantly in space. As a result, the geometrical domain decomposition in parallel reacting flow simulations leads to a high computational load imbalance. In that regard, an open-source dynamic load balancing algorithm [44] to speed up the reactive multiprocessor simulations was introduced, which is employed here. Further improvements regarding the total execution time could be reached by optimizing the cell-based chemistry ODE solution routines. Following this idea, an analytical Jacobian formulation provided by the open-source library pyJac was implemented in OpenFOAM, and the efficient linear algebra package LAPACK was utilized for faster chemistry solution [45], both included in the present numerical model.

2.3 Reactive Flow Field. The stabilization mechanism of the low-swirl lifted flame fundamentally differs from a high-swirl flow field which exhibits the vortex breakdown, being typical for state-of-the-art gas turbine combustors. In Fig. 5, the contour plots of the instantaneous axial velocity, the temperature and the OH mass fraction of the reactive flow field of the single-burner configuration are shown. In addition, the isoline of zero mean axial velocity $\langle u_x \rangle$ indicating recirculation areas, and isolines of the mean heat release rate $\langle \dot{\omega}_T \rangle$ representing the reaction zone are superimposed.

The turbulent swirling jet issued from the nozzle can be identified in the axial velocity and temperature field. Due to the entrainment of surrounding fluid by the confined jet flow, the ORZ of burned gases is formed in the combustor edge cavities. Consequently, hot combustion products are transported upstream, and mixed with the reactants, which is promoted by flow instabilities on the jet surface, controlling the ignition of the fresh mixture. Furthermore, it is evident that a dominant inner recirculation zone does not exist for this type of low-swirl configuration. Based on the heat release isolines, the characteristic arrow-shaped flame is visible which is anchored at the outer shear layer of the jet along the edge of the recirculation zone, as also observed in the previous numerical studies [27–29]. On the nozzle axis, the reaction zone is pushed downstream due to the high velocity in the core region of the swirling jet. Reaching quasi-premixed conditions at the position of stabilization, the flame front is propagating against the incoming flow. Hence, the lifted flame is stabilized in the high-velocity flow field of the swirling jet where an equilibrium between the burning velocity and the flow velocity is reached [19,46].

The predicted field of the OH mass fraction shows good agreement with the experiment in terms of the measured planar OH-LIF (see Fig. 3). In the premixing zone upstream of the flame, OH can be found in the jet shear layer due to the mixing with the hot combustion products, leading to locally reacting fresh-gas mixtures. In the main reaction zone, the highest concentrations of OH are present. There are also reactive pockets visible which are transported further downstream from the flame front, similar to experimental observations.

For a more detailed comparison of the flame characteristics, the measured OH* chemiluminescence map, and the postprocessed fields of the predicted heat release and OH* mass fraction as line-of-sight integrations are shown in Fig. 6, including the corresponding LOH. In the case of OH*, the indicated main combustion zone is shifted downstream compared to the equivalent zone in the line-of-sight integrated heat release map, increasing the predicted LOH. This is in accordance with the experimental findings of Lauer and Sattelmayer [47], in which a downstream shift in OH* chemiluminescence intensity were reported based on the distribution of the heat release rate. As it can be seen, the position of the flame leading edge is well predicted by the simulation since the LOH is close to the experimental value. However, the axial and radial flame extent are slightly underestimated by the numerical predictions. The final thermochemical state of the reacting flow is correctly predicted, as demonstrated by the comparison of the temperature and species mass fractions at the combustor outlet with calculations performed with the software toolkit Cantera using a detailed chemical mechanism, not shown here.

To summarize the investigation of the low-swirl lifted flame, it is shown that the developed numerical model adequately reproduces the underlying physics of this type of flame. By using inlet profiles for the velocity components coupled with the inflow-turbulence generator, the characteristic flow field of the low-swirl jet inside the combustor is captured correctly. The LOH is well predicted, which is generally a severe test for partially premixed combustion models due to intense turbulence attributed to the high shear in the jet [46]. The reaction mechanism and the combustion model employed provide good accuracy regarding the involved chemical kinetics and

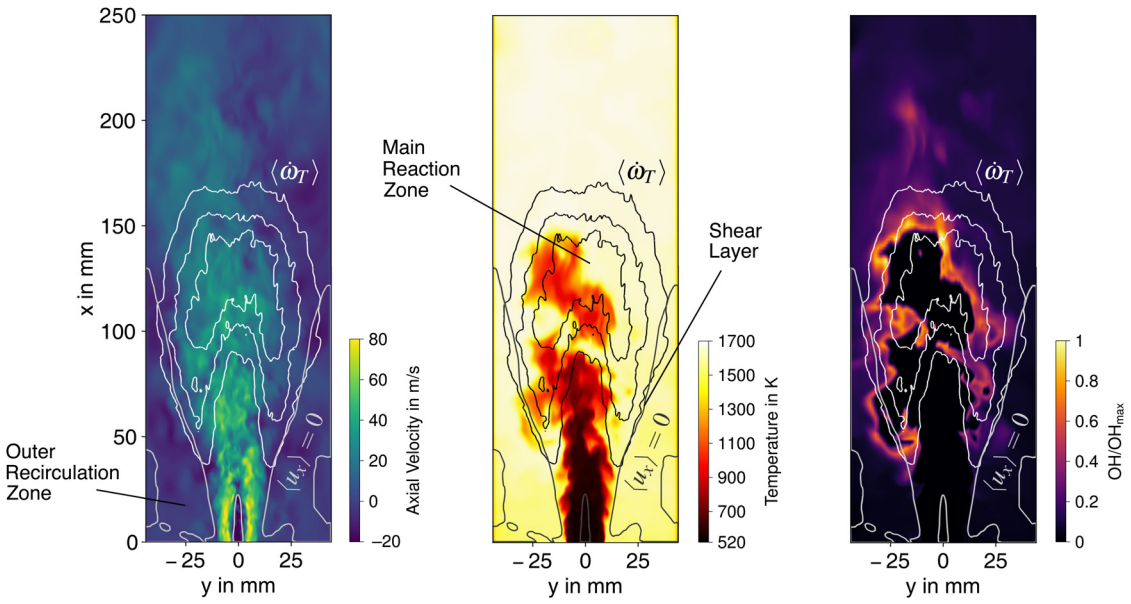

Fig. 5 Contour plots of the instantaneous fields of axial velocity (left), temperature (middle), and OH mass fraction (right) for the single-burner

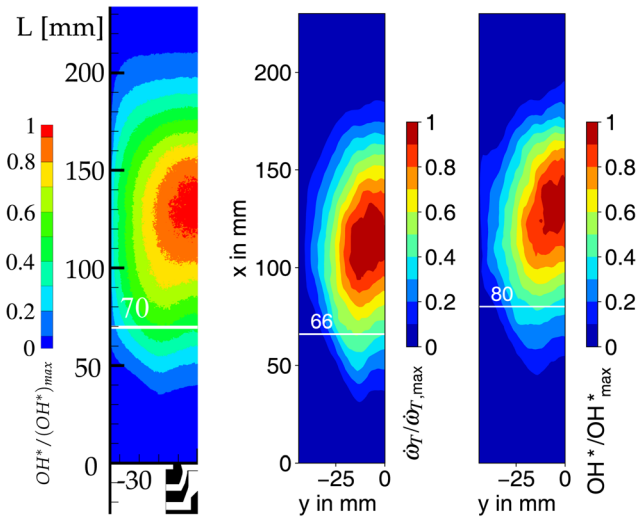

Fig. 6 Comparison of the experimental OH* emission intensity (left) adapted from Ref. [26] to the line-of-sight integrations of the heat release (middle) and OH* mass fraction (right)

turbulence–chemistry interaction of the kinetically controlled flame featuring a low Damköhler number smaller than unity [23]. On the basis of the results accomplished in this section, the numerical model is conclusively validated since it captures the main features of turbulent mixing and finite-rate chemistry, governing the lifted flame characteristics. Hence, the model is used in Sec. 3 of the paper, addressing the reacting flow prediction of the tilted SHC burner arrangement.

The observed differences to the experiment regarding the flame extent can be attributed to the uncertainty in the distribution of the wall heat losses, affecting the combustor temperature, and thus chemical reaction rates of the flame. The evaluation of the chemical and mixing time scale, which are key in the formulation of the PaSR model, could also be revised in future works.

3 Short Helical Combustor Reacting Flow Prediction

As elucidated in Sec. 2, the stabilization of the lifted flame relies on the presence of the ORZ of entrained exhaust gases. Hence, it is crucial for the development of the annular SHC featuring the low-swirl burner to ensure the backflow of hot combustion products along the confining combustor walls. In that regard, the sidewall of the staggered nonsymmetrical SHC arrangement plays a decisive role as the only lateral flow confinement. The interaction of adjacent burners is investigated by means of reacting flow predictions. By the variation of the combustor confinement ratio, the impact on recirculation characteristics and the flame liftoff are discussed.

3.1 Numerical Model. A simplified burner of the annular combustor is used for the SHC reacting flow simulation. The generic geometry of two adjacent sectors of the SHC is shown in Fig. 7. It

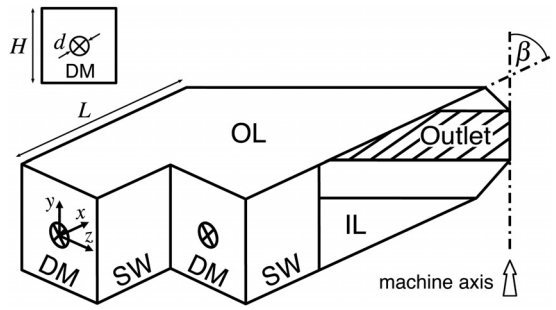

Fig. 7 Geometry of two generic SHC sectors. DM: dome, SW: sidewall, OL: outer liner, IL: inner liner.

highlights the three-dimensional staggered burner arrangement. The tilting angle of the burner axis with respect to the machine axis is $\beta = 45$ deg, as used for the investigation of the isothermal flow in the previous work of the authors [30]. In the computational model, the low-swirl nozzle is not included, similar to the previous validation study involving the enclosed single-burner configuration. However, the reference swirl nozzle used for the SHC is larger compared to the single-burner, featuring an effective area of 319 mm^2. This implies an increased size of the circular inlet patch which represents the outlet cross section of the larger nozzle. The computational mesh of one SHC sector representing the reference case consists of 2.8 M elements, predominantly hexahedral cells, and the averaging time for all configurations investigated is not less than 50 ms.

At the inlet patch, the time-averaged profiles of velocity, species mass fractions, and temperature (see Fig. 4) are prescribed. The larger nozzle of the SHC results from an up-scaling of the nozzle used by Sedlmaier et al. [20], preserving geometric similarity. Since the same relative pressure drop of 3% is assumed for the SHC, Mach number similarity is ensured. Hence, it is assumed that under the same operating conditions, all profiles of the similar nozzles can be regarded as qualitatively the same. To take account of the increased mass flowrate through the larger nozzle due to the higher effective area, the inlet profiles of the three velocity components are scaled up by the ratio of the discharge coefficients of both swirlers, also done in the previous numerical studies [31,32]. The synthetic inflow-turbulence generator is employed to impose turbulent fluctuations at the inlet, and the wall-adapting local eddy-viscosity subgrid-scale model is used.

The same operating conditions with respect to the air preheating temperature, pressure, and equivalence ratio are chosen for the SHC. The no-slip condition is enforced at the walls. Furthermore, all combustor walls are considered to be adiabatic. In the single-burner experiment [26], it was shown that the flame LOH increases for higher wall heat losses due to a reduction of the combustor temperature, and thus lower reaction rates. Since this conceptual study is focused on the general understanding of the SHC characteristics, the effects of wall heat losses on the hot-gas recirculation is neglected, which would presumably only cause a downstream shift in flame position. By using translational periodic boundary conditions in circumferential direction, the interaction of adjacent low-swirl flames is taken into account. Concerning the chemical kinetics and turbulence–chemistry interaction, the extended KEE reaction mechanism including OH* formation and the PaSR combustion model are used.

3.2 Reference Configuration. In this section, the results of the reacting flow simulation of the SHC reference configuration are presented. The nozzle diameter d and the overall combustor dimensions, $H = 100$ mm and $L = 300$ mm (see Fig. 7), are defined to correspond to the test rig of the experimental studies performed within the same EU-funded research project [31]. The reference case features a confinement ratio between the flame tube height H and the nozzle diameter d of $R_C^{REF} = H/d = 4$.

In Fig. 8, the contour plots of the instantaneous axial velocity, the temperature, and the OH mass fraction of the reacting flow are shown in the SHC midplane, with isolines of time-averaged zero axial velocity and heat release being superimposed. The reactive flow field of the SHC is overall resembling the characteristics of the single-burner configuration (see Fig. 5). Reactive pockets indicated by the formation of OH can be observed up- and downstream of the main combustion zone, and the surface of the swirling jet shows instabilities attributed to the high shear stresses. The low-swirl jet consisting of fresh mixture is interacting with the hot reaction products entrained from its surroundings, and mixed into the jet. However, the ORZ in the SHC is mainly occurring in the vicinity of the sidewall due to the nonsymmetrical arrangement of the confining combustor walls. This means a significant difference to the enclosed single-burner where recirculation zones are established entirely around the jet flow. Furthermore, the flow is deflected toward the combustor sidewall which is indicated by the mean velocity vector

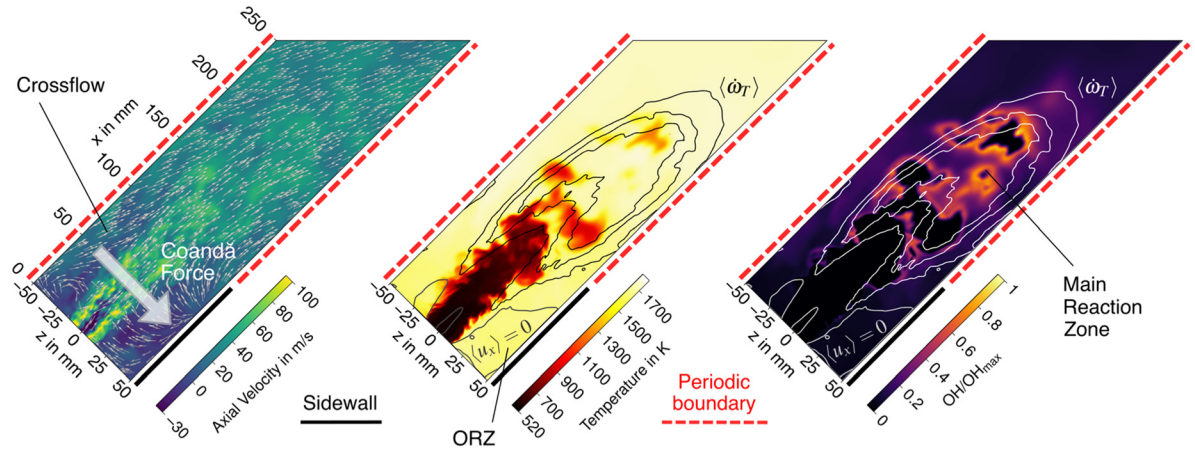

Fig. 8 Contour plots of the instantaneous fields of axial velocity (left), temperature (middle), and OH mass fraction (right) for the SHC reference case. Arrow indicates the direction of the deflecting force.

field. The mechanism leading to this deflection of the low-swirl jet is related to the Coandă effect, which was found in the previous aerodynamic investigations [30]. Near the sidewall, the pressure decrease in the vicinity of the jet caused by the entrainment of surrounding gas is enforced. This leads to a pressure difference across the jet, which exerts a force on the flow (see Fig. 8), causing the jet to be deflected toward the sidewall. As a result, a crossflow of hot products entering the burner on the open side is formed. The crossflow effect promotes exhaust gas recirculation between neighbor flames, and could compensate the reduced backflow of burned gases on this side.

By means of the line-of-sight integration of the mean OH* mass fraction indicating the combustion zone, the lifted flame is visualized in Fig. 9. It can be seen that the flame is not aligned with the burner axis, but it is deflected toward the combustor sidewall, which emphasizes the interaction with the neighbor flames. Concerning the shape of the flame, the reaction zone is narrower and more elongated in axial direction compared to the single-burner configuration. This is likely attributed to the entrainment of fluid from the adjacent sector, forming the crossflow which stretches the flame along the streamwise direction. Most importantly, it is to mention that the LOH is significantly increased in the SHC burner arrangement compared to the single-burner. This can be

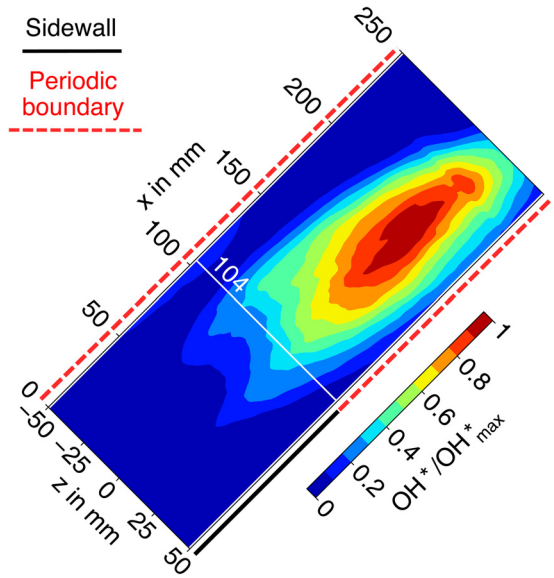

Fig. 9 Line-of-sight integration of the OH* mass fraction for the SHC reference case

explained with the higher nozzle outlet velocity and, hence, higher jet flow velocity which the propagating premixed-like flame front has to counteract for the stabilization at the equilibrium position. Consequently, the flame stability in terms of the LBO limit may decrease by using the larger nozzle [19].

3.3 Impact of Confinement Ratio. The confinement ratio between the combustor and the nozzle is an important parameter of technical combustion applications, determining the expansion rate of the swirl flow emerging from the nozzle. The impact of the confinement level has been addressed in several experimental studies of lean combustion systems featuring single swirl-stabilized flames. In these works, the flame-wall interaction was investigated, finding that the flame structure, heat release, and instability characteristics are affected by the flow confinement [48,49]. It was also concluded that an optimal confinement ratio exists, minimizing combustion emissions [50]. However, the asymmetric and tilted SHC arrangement including the interaction of adjacent flames in an annular concept differs from such single-flame setups. It was shown by the authors [30] that the ORZ of the isothermal jet flow in the SHC design significantly increases in size for a larger cross-sectional area of the burner. Following this result, the impact of the geometric confinement on the lifted flame of the reactive case is discussed as a possible concept optimization.

In this work, the confinement ratio is defined as the ratio between the combustor height H and the outlet nozzle diameter d. In addition to the reference case ($R_C^{\mathrm{REF}} = 4$) studied in Sec. 3.2, the confinement ratio is reduced as well as increased to values of $R_C = 3$, 5, and 6. The combustor height and width are both scaled by the same ratio when the confinement is varied, preserving the quadratic shape of the flame tube. The nozzle diameter d and the combustor length L remain constant. It is to be noted that for a burner tilting angle of 45 deg, the sidewall length is equal to the flame tube height and width.

The instantaneous axial velocity and temperature fields of the differently confined low-swirl flames in the SHC midplane are shown in Fig. 10. It can be seen that all configurations exhibit the similar characteristics of the high-velocity swirling jet entering the combustor. The jet comprises the nonswirling outer flow which encloses the inner swirling part, preventing a sudden radial expansion. However, the recirculation of burned gases is different when comparing all cases, with the size of the ORZ considerably increasing for higher confinement ratios. This is due to the higher combustor volume providing more space for the backflow of combustion products. For $R_C = 6$, the volume of the recirculation zone V_{rec} is 3.7 times higher compared to the reference case of $R_C^{\mathrm{REF}} = 4$, which is graphically shown in Fig. 11. The combustion products are mainly recirculating along the SHC sidewall, as

indicated by the isoline of zero mean axial velocity, and observed before for the reference case. In the temperature contour plots, the turbulent instabilities on the jet surface indicate the mixing between the fresh and burned gases, ensuring the preheating of the mixture. For the smallest confinement ratio of $R_C = 3$, the deflection of the jet flow toward the sidewall is very pronounced. The flame reaches across the periodic boundary of the sector, and thus merged reaction zones of adjacent burners are formed which is concluded from the isolines of the heat release rate. In case of the largest flame tube featuring $R_C = 6$, the main reaction zone is more elongated along the burner axis compared to the reference case. Besides the volume of the ORZ, the temperature of recirculating hot gases is affected as well by the combustor confinement. It is found that the volume-averaged temperature of the ORZ $\bar{T}_{\text{rec}}$ is 1712 K for the largest flame tube, in contrast to 1656 K for the reference case and only 1582 K for $R_C = 3$ (see Fig. 11). The present understanding is that the increasing ORZ temperature of the larger combustors can be explained with the higher residence time of the hot gases between adjacent sectors due to the higher distance in circumferential direction between the burners. This increases the temperature of the combustion products before recirculating at the sidewall in the neighbor sector due to the crossflow effect.

For further analyzing the lifted flames of different confinement ratios, the time-averaged OH* line-of-sight integrations are presented in Fig. 12 also reporting the LOH. Decreasing the confinement ratio reduces the distance between the burners. Hence, the interaction of adjacent low-swirl flows increases, which can be distinctly seen for the smallest flame tube cross section investigated ($R_C = 3$), leading to the reaction zones being strongly distorted, and connected with each other. For this configuration, no LOH is indicated because the value would be misleading caused by the advection of OH* from the neighboring sector. The higher confinement ratios reveal nearly the same stabilization point, with the LOH being stable at around 100 mm. However, it appears that by increasing the flame tube size, the flame shape becomes more asymmetrical, with the reaction rates being enforced near the combustor sidewall. This could be attributed to the larger recirculation zone, and thus the more pronounced shear layers anchoring the flame front (see Fig. 10).

3.4 Final Remarks. In the staggered SHC burner arrangement, the flow field is highly complex and three-dimensional, featuring the

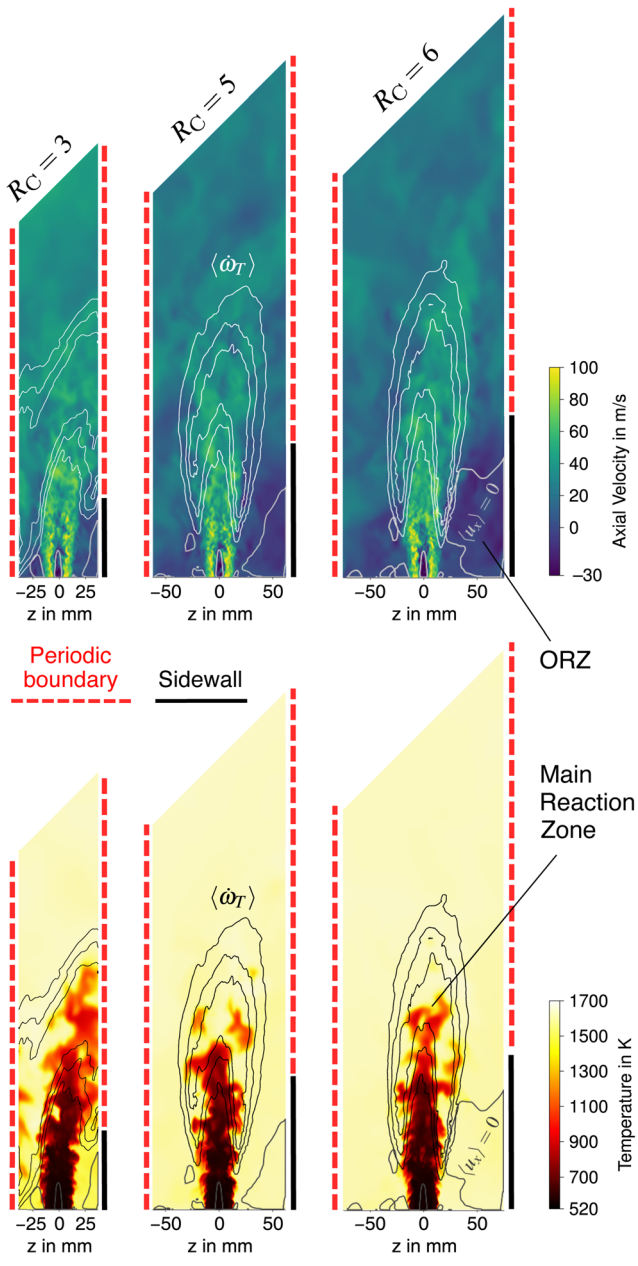

Fig. 10 Contour plots of the instantaneous fields of axial velocity (top) and temperature (bottom) for different confinement ratios of the SHC

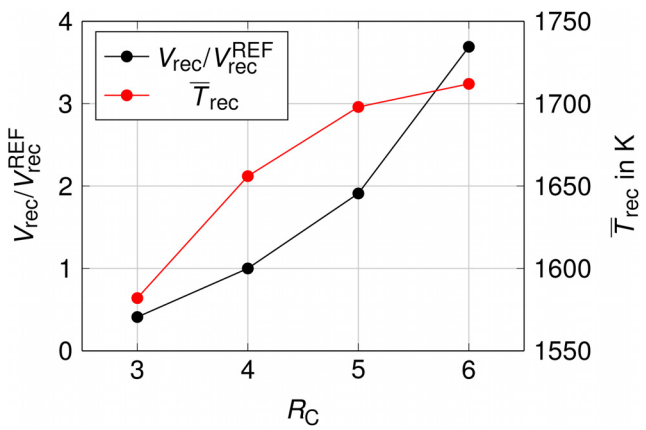

Fig. 11 Volume and volume-averaged temperature of the outer recirculation zone over the confinement ratio

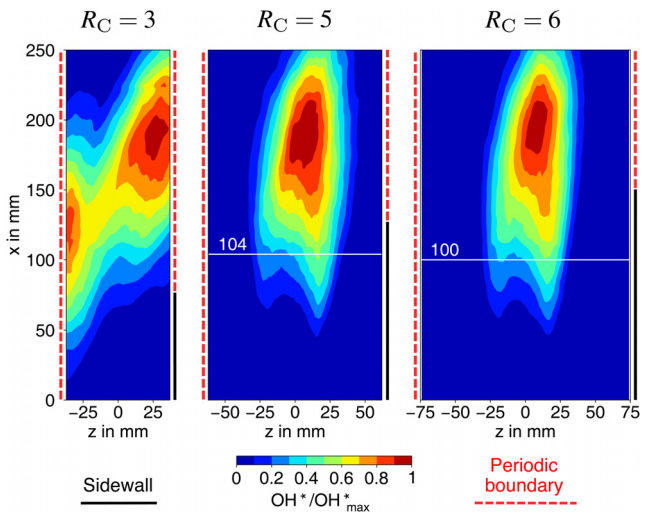

Fig. 12 Line-of-sight integrations of the OH* mass fraction for different confinement ratios of the SHC

interaction of adjacent burners by the formation of a crossflow of hot combustion products. Similar to the results of this work, a significant increase of the size of the ORZ was also observed by Langone et al. [32] by the variation of the burner tilting angle, but not affecting the LOH. Hence, it could be concluded that the extent of the ORZ in the SHC has a minor impact on the flame stabilization position, which needs to be substantiated by further investigations. However, the LOH is only one indicator of flame stability, with a large hot-gas reservoir of vitiated combustion products and the outer shear layers contributing to the stabilization process.

4 Conclusion

In this work, the novel design of a lean partially premixed aero engine combustor is investigated. The concept consists of the tilted burner arrangement of the SHC, and the combustion technique involving lifted flames based on specific low-swirl injector nozzles. This configuration promises ultralow NO_x emissions due to fuel–air premixing, while ensuring safe and stable operation without requiring a diffusive pilot flame for stabilizing the main lean flame.

Based on LES reacting flow predictions of the lifted flame in a preliminary study, the dedicated numerical model is validated against experimental measurements of a laboratory combustor rig. It is demonstrated that by using the finite-rate chemistry approach, the setup is capable of reproducing the features governing the flame characteristics adequately.

The numerical simulation of the low-swirl lifted flame in the SHC arrangement shows that the jet flow is deflected toward the lateral sidewall of the staggered combustor dome. This is attributed to an asymmetric pressure field in the vicinity of the burner. As a result, a crossflow of burned gases between adjacent combustor sectors is established, promoting the exhaust gas recirculation, which is the main stabilization mechanism of the flame. The majority of the outer recirculation zone is situated along the sidewall, which leads to a highly complex three-dimensional flow field pattern.

By varying the confinement ratio, the impact of the combustor size on the recirculation process and the flame liftoff height is studied. It is shown that the flame position is not significantly affected, yet the size and the volume-averaged temperature of the recirculation zone strongly increase for larger flame tubes. For a reduced confinement ratio, and thus a smaller distance between neighboring burners, the adjacent flames merge, forming an interrelated reaction zone.

In a future parametric study of the SHC concept, the impact of other design features, e.g., the burner tilting angle, will be evaluated. Furthermore, the numerical model will be extended by the prediction of NO_x formation in order to compare different SHC geometries with respect to the emission reduction potential.

Acknowledgment

This project has received funding from the Clean Sky 2 Joint Undertaking (JU) under Grant Agreement No. 831881 (CHAiR-LIFT). The JU receives support from the European Union's Horizon 2020 research and innovation programme and the Clean Sky 2 JU members other than the Union.

The numerical computations were performed on the high performance computing cluster bwUni-Cluster at the Karlsruhe Institute of Technology. The HPC resource bwUniCluster is funded by the Ministry of Science, Research and the Arts Baden Württemberg and the DFG ("Deutsche Forschungsgemeinschaft"). The authors acknowledge support by the state of Baden-Württemberg through bwHPC.

Funding Data

- Clean Sky 2 Joint Undertaking (JU) (Grant Agreement No. 831881; Funder ID: 10.13039/501100006221).

Data Availability Statement

The datasets generated and supporting the findings of this article are obtainable from the corresponding author upon reasonable request.

Nomenclature

Symbols

d = nozzle diameter
H = combustor height
L = combustor length
p = pressure
R_C = confinement ratio
T = temperature
$\bar{T}_{\mathrm{rec}}$ = temperature of the recirculation zone
u_i = velocity vector
V_{rec} = volume of the recirculation zone
x, y, z = Cartesian coordinates
Y_k = species mass fraction
β = burner tilting angle
$\Delta p/p_0$ = relative pressure drop
κ = reacting volume fraction
τ_c = chemical time scale
τ_{mix} = mixing time scale
ϕ = equivalence ratio
$\dot{\omega}_k$ = species formation rate
$\dot{\omega}_T$ = heat release rate

Abbreviations

CFD = computational fluid dynamics
LBO = lean blow-out
LES = large eddy simulation
LOH = liftoff height
LPP = lean premixed prevaporized
ODE = ordinary differential equation
ORZ = outer recirculation zone
PaSR = partially stirred reactor
SHC = short helical combustor

References

[1] European Commission, 2011, "Flightpath 2050: Europe's Vision for Aviation," Publications Office of the European Union, Luxembourg City, Luxembourg.
[2] Lieuwen, T. C., and Yang, V., eds., 2013, *Gas Turbine Emissions*, Cambridge University Press, New York.
[3] Bauer, H.-J., 2004, "New Low Emission Strategies and Combustor Designs for Civil Aeroengine Applications," Prog. Comput. Fluid Dyn., **4**(3–5), pp. 130–142.
[4] Liu, Y., Sun, X., Sethi, V., Nalianda, D., Li, Y.-G., and Wang, L., 2017, "Review of Modern Low Emissions Combustion Technologies for Aero Gas Turbine Engines," Prog. Aerosp. Sci., **94**, pp. 12–45.
[5] Ranasinghe, K., Guan, K., Gardi, A., and Sabatini, R., 2019, "Review of Advanced Low-Emission Technologies for Sustainable Aviation," Energy, **188**, p. 115945.
[6] Tacina, R. R., 1990, "Low NO_x Potential of Gas Turbine Engines," AIAA Paper No. 90-0550.
[7] Lefebvre, A. H., and Ballal, D. R., 2010, *Gas Turbine Combustion: Alternative Fuels and Emissions*, 3rd ed., CRC Press, Boca Raton, FL.
[8] Ariatabar, B., 2019, "Aerothermal Analysis of an Aeroengine Annular Combustor Concept With Angular Air Supply," Ph.D. thesis, Fakultät für Maschinenbau, Karlsruher Institut für Technologie (KIT), Karlsruhe, Germany.
[9] Ariatabar, B., Koch, R., Bauer, H.-J., and Negulescu, D.-A., 2016, "Short Helical Combustor: Concept Study of an Innovative Gas Turbine Combustor With Angular Air Supply," ASME J. Eng. Gas Turbines Power, **138**(3), p. 031503.
[10] Ariatabar, B., Koch, R., and Bauer, H.-J., 2017, "Short Helical Combustor: Dynamic Flow Analysis in a Combustion System With Angular Air Supply," ASME J. Eng. Gas Turbines Power, **139**(4), p. 041505.
[11] Ariatabar, B., Koch, R., and Bauer, H.-J., 2018, "Short Helical Combustor: Flow Control in a Combustion System With Angular Air Supply," ASME J. Eng. Gas Turbines Power, **140**(3), p. 031507.
[12] Hu, B., Zhang, J., Deng, A., Zhao, W., and Zhao, Q., 2018, "Numerical Investigation on Single-Restricted Swirling Flows in an Innovative Combustor," ASME Paper No. GT2018-76000.
[13] Fric, T. F., 1993, "Effects of Fuel-Air Unmixedness on NO_x Emissions," J. Propul. Power, **9**(5), pp. 708–713.
[14] Pitts, W. M., 1989, "Assessment of Theories for the Behavior and Blowout of Lifted Turbulent Jet Diffusion Flames," Symp. (Int.) Combust., **22**(1), pp. 809–816.

[15] Lyons, K. M., 2007, "Toward an Understanding of the Stabilization Mechanisms of Lifted Turbulent Jet Flames: Experiments," Prog. Energy Combust. Sci., **33**(2), pp. 211–231.
[16] Lawn, C. J., 2009, "Lifted Flames on Fuel Jets in Co-Flowing Air," Prog. Energy Combust. Sci., **35**(1), pp. 1–30.
[17] Cheng, R. K., 2006, "Low Swirl Combustion," *The Gas Turbine Handbook*, R. Dennis, ed., U.S. Department of Energy, National Energy Technology Laboratory, Morgantown, WV, pp. 241–254.
[18] Fokaides, P. A., Kasabov, P., and Zarzalis, N., 2008, "Experimental Investigation of the Stability Mechanism and Emissions of a Lifted Swirl Nonpremixed Flame," ASME J. Eng. Gas Turbines Power, **130**(1), p. 011508.
[19] Kasabov, P., Zarzalis, N., and Habisreuther, P., 2013, "Experimental Study on Lifted Flames Operated With Liquid Kerosene at Elevated Pressure and Stabilized by Outer Recirculation," Flow, Turbul. Combust., **90**(3), pp. 605–619.
[20] Sedlmaier, J., Habisreuther, P., Zarzalis, N., and Jansohn, P., 2014, "Influence of Liquid and Gaseous Fuel on Lifted Flames at Elevated Pressure Stabilized by Outer Recirculation," ASME Paper No. GT2014-25823.
[21] Zarzalis, N., Fokaides, P., and Merkle, K., 2006, "Fuel Injection Apparatus," European Patent No. 1 722 164 A1.
[22] Kasabov, P., and Zarzalis, N., 2009, "Pressure Dependence of the Stability Limits and the NO_x Exhaust Gas Concentrations in Case of Swirl-Stabilized, Diffusion Flames Burning in a Lift-Off Regime," ASME Paper No. GT2009-59801.
[23] Kasabov, P., 2014, "Experimentelle Untersuchungen an Abgehobenen Flammen Unter Druck," Ph.D. thesis, Fakultät für Chemieingenieurwesen und Verfahrenstechnik, Karlsruher Institut für Technologie (KIT), Karlsruhe, Germany.
[24] Gicquel, L. Y. M., Staffelbach, G., and Poinsot, T., 2012, "Large Eddy Simulations of Gaseous Flames in Gas Turbine Combustion Chambers," Prog. Energy Combust. Sci., **38**(6), pp. 782–817.
[25] Kern, M., Fokaides, P., Habisreuther, P., and Zarzalis, N., 2009, "Applicability of a Flamelet and a Presumed JPDF 2-Domain-1-Step-Kinetic Turbulent Reaction Model for the Simulation of a Lifted Swirl Flame," ASME Paper No. GT2009-59435.
[26] Sedlmaier, J., 2019, "Numerische Und Experimentelle Untersuchung Einer Abgehobenen Flamme Unter Druck," Ph.D. thesis, Fakultät für Chemieingenieurwesen und Verfahrenstechnik, Karlsruher Institut für Technologie (KIT), Karlsruhe, Germany.
[27] Langone, L., Sedlmaier, J., Nassini, P. C., Mazzei, L., Harth, S., and Andreini, A., 2020, "Numerical Modeling of Gaseous Partially Premixed Low-Swirl Lifted Flame at Elevated Pressure," ASME Paper No. GT2020-16305.
[28] Langone, L., Amerighi, M., and Andreini, A., 2022, "Large Eddy Simulations of a Low-Swirl Gaseous Partially Premixed Lifted Flame in Presence of Wall Heat Losses," Energies, **15**(3), p. 788.
[29] Langone, L., Amerighi, M., Mazzei, L., Andreini, A., Orsino, S., Ansari, N., and Yadav, R., 2022, "Assessment of Thickened Flame Model Coupled With Flamelet Generated Manifold on a Low-Swirl Partially Premixed Gaseous Lifted Flame," ASME Paper No. GT2022-82122.
[30] Hoffmann, S., Koch, R., and Bauer, H.-J., 2021, "Numerical Investigation of the Low-Swirl Flow in an Aeronautical Combustor With Angular Air Supply," ASME Paper No. GT2021-59286.
[31] Shamma, M., Hoffmann, S., Harth, S. R., Zarzalis, N., Trimis, D., Koch, R., Bauer, H.-J., Langone, L., Galeotti, S., and Andreini, A., 2021, "Investigation of Adjacent Lifted Flames Interaction in an Inline and Inclined Multi-Burner Arrangement," ASME Paper No. GT2021-59941.
[32] Langone, L., Amerighi, M., and Andreini, A., 2022, "Numerical Modeling of Lean Spray Lifted Flames in Inclined Multi-Burner Arrangements," ASME Paper No. GT2022-82102.
[33] Gupta, A. K., Lilley, D. G., and Syred, N., 1984, *Swirl Flows*, Abacus Press, Tunbridge Wells, Kent, UK.
[34] Greenshields, C., 2019, *OpenFOAM v7 User Guide*, The OpenFOAM Foundation, London, UK.
[35] Tabor, G. R., and Baba-Ahmadi, M. H., 2010, "Inlet Conditions for Large Eddy Simulation: A Review," Comput. Fluids, **39**(4), pp. 553–567.
[36] Galeazzo, F. C. C., Zhang, F., Zirwes, T., Habisreuther, P., Bockhorn, H., Zarzalis, N., and Trimis, D., 2021, "Implementation of an Efficient Synthetic Inflow Turbulence-Generator in the Open-Source Code Openfoam for 3D LES/DNS Applications," *High Performance Computing in Science and Engineering '20*, W. E. Nagel, D. H. Kröner, and M. M. Resch, eds., Springer, Cham, Switzerland, pp. 207–221.
[37] Klein, M., Sadiki, A., and Janicka, J., 2003, "A Digital Filter Based Generation of Inflow Data for Spatially Developing Direct Numerical or Large Eddy Simulations," J. Comput. Phys., **186**(2), pp. 652–665.
[38] Nicoud, F., and Ducros, F., 1999, "Subgrid-Scale Stress Modelling Based on the Square of the Velocity Gradient Tensor," Flow, Turbul. Combust., **62**(3), pp. 183–200.
[39] Kee, R. J., Grcar, J. F., Smooke, M. D., and Miller, J. A., 1985, "A Fortran Program for Modeling Steady Laminar One-Dimensional Premixed Flames," Sandia National Laboratories, Albuquerque, NM, Report No. SAND85-8240.
[40] Kathrotia, T., 2011, "Reaction Kinetics Modeling of OH*, CH*, and C2* Chemiluminescence," Ph.D. thesis, Naturwisschenschaftlich-Mathematische Gesamtfakultät, Ruprecht-Karls-Universität, Heidelberg, Germany.
[41] Chomiak, J., 1990, *Combustion: A Study in Theory, Fact and Application*, Abacus Press, New York.
[42] Li, Z., Ferrarotti, M., Cuoci, A., and Parente, A., 2018, "Finite-Rate Chemistry Modelling of Non-Conventional Combustion Regimes Using a Partially-Stirred Reactor Closure: Combustion Model Formulation and Implementation Details," Appl. Energy, **225**, pp. 637–655.
[43] Ferrarotti, M., Li, Z., and Parente, A., 2019, "On the Role of Mixing Models in the Simulation of Mild Combustion Using Finite-Rate Chemistry Combustion Models," Proc. Combust. Inst., **37**(4), pp. 4531–4538.
[44] Tekgül, B., Peltonen, P., Kahila, H., Kaario, O., and Vuorinen, V., 2021, "DLBFoam: An Open-Source Dynamic Load Balancing Model for Fast Reacting Flow Simulations in OpenFOAM," Comput. Phys. Commun., **267**, p. 108073.
[45] Morev, I., Tekgül, B., Gadalla, M., Shahanaghi, A., Kannan, J., Karimkashi, S., Kaario, O., and Vuorinen, V., 2022, "Fast Reactive Flow Simulations Using Analytical Jacobian and Dynamic Load Balancing in OpenFOAM," Phys. Fluids, **34**(2), p. 021801.
[46] Peters, N., 2004, *Turbulent Combustion*, Cambridge University Press, Cambridge, UK.
[47] Lauer, M., and Sattelmayer, T., 2010, "On the Adequacy of Chemiluminescence as a Measure for Heat Release in Turbulent Flames With Mixture Gradients," ASME J. Eng. Gas Turbines Power, **132**(6), p. 061502.
[48] De Rosa, A. J., Peluso, S. J., Quay, B. D., and Santavicca, D. A., 2015, "The Effect of Confinement on the Structure and Dynamic Response of Lean-Premixed, Swirl-Stabilized Flames," ASME Paper No. GT2015-42178.
[49] Tong, Y., Li, M., Thern, M., and Klingmann, J., 2017, "An Experimental Study of Effects of Confinement Ratio on Swirl Stabilized Flame Macrostructures," ASME Paper No. POWER-ICOPE2017-3064.
[50] Zeng, Q., Kong, W., and Sui, C., 2013, "Effect of Confinement on Combustion Characteristics in Lean Direct Injection Combustion System," ASME Paper No. GT2013-95413.